

## FFAG for High Intensity Proton Accelerator

Y. Mori

*Kyoto University, Research Reactor Institute,  
Kumatori, Osaka 590-0494, Japan*

*\* E-mail: mori@rri.kyoto-u.ac.jp  
www.rri.kyoto-u.ac.jp/*

Fixed Field Alternating Gradient accelerators(FFAGs) have been developed for various applications recently. Contrary to the ordinary synchrotron, FFAGs have a large capability of accelerating high current beams because of strong beam focusing to have a large beam acceptance and static magnetic field which allows to have very fast beam acceleration and large repetition rate in operation. In this paper I will present the expected characteristics and possible performance of FFAG as the proton drivers for ADSR and muon source, and also show the recent preliminary experiment on ADSR with FFAG proton accelerator complex at Kyoto University Research Reactor Institute (KURRI).

*Keywords:* FFAG;ADSR

### 1. Introduction

The idea of FFAG accelerator was originally invented by Ohkawa in 1953<sup>1</sup> and also by Symon and Kolomenskii, independently. Electron models of FFAG accelerator have been built by Kerst, Cole and Symon at MURA in the early 1960s.<sup>2</sup> However, since then, no FFAG proton accelerator has been built until recently. A proton FFAG accelerator, in particular, has some severe technical difficulties such as its complicated configuration of magnetic field and difficulty of rf acceleration. In 2000, the world's first proton FFAG accelerator (POP-FFAG) was demonstrated using a novel broad-band RF cavity with high permeability MA(magnetic alloy) cores at KEK.<sup>3</sup> Following this success, it has been recognized that FFAGs have large advantages in rapid acceleration with large momentum acceptance, which are useful both for muon accelerators and for high power proton drivers. Since then, intensive studies and discussions have been made, and various works for the development of FFAGs have also started for many applications at many institutes. The FFAG accelerator has distinctive features compared with

other types of accelerators in beam focusing and acceleration. In transverse beam focusing, two types of beam focusing can be categorized: scaling and non-scaling. The scaling type of FFAG accelerator has non-chromatic beam optics in which a large amount of non-linear field is essential. In the non-scaling type of FFAG accelerator, fields are linear. However, a number of betatron resonances have to be crossed during acceleration. As for beam acceleration, various schemes with new ideas such as broad-band MA rf cavity, stationary bucket acceleration, serpentine acceleration and harmonic number jump acceleration have been studied intensively and some of them have been realized.

## 2. Beam focusing and acceleration in FFAG accelerator

### 2.1. Beam focusing

#### 2.1.1. Scaling

In the scaling type of FFAG accelerator, each beam orbit for different beam momentum has similarity in shape (curvature), and zero chromaticity in the beam optics is realized. Thus, the betatron tunes for both horizontal and vertical directions keep constant during beam acceleration without any problems caused by resonance crossing. The transverse linearized betatron equation of motion can be expressed by the following equation.

$$\frac{d^2 X}{ds^2} + K(s)X = 0, \quad (1)$$

where  $s$  is the distance along the reference trajectory and  $K(s)$  can be given for horizontal ( $x$ ) and vertical ( $z$ ) directions by,

$$K_x = \frac{1 - n(s)}{\rho^2(s)} \quad (2)$$

$$K_z = -\frac{n(s)}{\rho^2(s)}, \quad (3)$$

respectively. Here  $n$  is a field index,

$$n = -\frac{\rho}{B}. \quad (4)$$

The scaling condition requires that the equation of motion of eq.(1) is independent of momentum both for horizontal and vertical directions, respectively. In cylindrical coordinates,

$$r = \rho$$

$$\frac{r}{B} \left( \frac{B_z}{z} \right)_{z=0} = k. \quad (5)$$

It can be shown analytically that the configuration of the magnetic field at the median plane can be expressed in the following equation including azimuthal direction.<sup>4</sup>

$$B(r, \theta) = B_0 \left( \frac{r}{r_0} \right)^k f \left( \theta - \zeta \ln \frac{r}{r_0} \right) \quad (6)$$

where  $\zeta = \tan \xi$ , and  $\xi$  is a spiral angle of the magnet in the azimuth plane. Accordingly, two schemes for beam focusing are invoked by this magnetic field configuration: one is radial sector focusing and the other spiral sector focusing. Radial sector focusing uses a combination of positive and negative bending magnets to make strong beam focusing with a FODO lattice configuration. In spiral sector focusing, edge focusing is used efficiently.

### 2.1.2. *Non-scaling*

The non-scaling type of FFAG accelerator has a basically simple structure composed of linear optical elements such as dipole and quadrupole magnets. The transverse betatron tune, however, is not constant during acceleration and fast acceleration is essential in the non-scaling type of FFAG accelerator to avoid beam losses caused by resonance crossing. To ensure this, the RF cavity phases are fixed for beam acceleration and the range of times-of-flight over the energy range of the accelerator is minimized when the path length difference has a parabolic dependence on beam momentum. In Fig. 1, a typical cell structure of a non-scaling FFAG accelerator are presented.<sup>5</sup> Based on the concept of linear non-scaling FFAG accelerators, some variations such as isochronous or semi-achromatic lattice<sup>6,7</sup> including small non-linear elements (semi-scaling) have also been proposed.

### 2.1.3. *Advancements of scaling FFAG optics*

Scaling law of FFAG accelerator to satisfy the zero chromaticity is used to be applied to circular accelerator as described above and each cell provides a total bending angle of a ring. If a scaling FFAG unit cell with straight line where a overall bending angle is zero is created, insertion/matching optics with straight lines can be cooperated to the ordinary FFAG ring. The

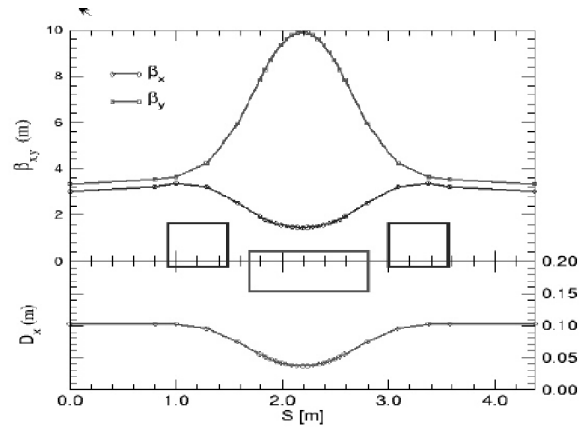


Fig. 1. Typical cell structure of a non-scaling FFAG accelerator are presented.

scaling condition for the straight line unit cell, i.e. a same phase advance per cell at every energy, leads to a different field law as shown below.

$$\frac{d\left(\frac{1}{\rho^2}\right)}{dp} = 0 \quad (7)$$

$$\frac{d(K\rho^2)}{dp} = 0 \quad (8)$$

Geometrical similarity is given by  $\rho = \text{const.}$  and it leads to a solution for magnetic field configuration.<sup>8</sup>

$$B_z = B_0 \exp\left(\frac{n}{\rho}(X-X_0)\right) \quad (9)$$

With a scaling FFAG straight line, insertion/matching optics to the ordinary scaling FFAG rings have been examined for various applications.<sup>9,10</sup> Figure 2 shows one of the examples for the dispersion suppressing insertion of the muon FFAG ring which is designed to accelerate muons up to 10GeV.<sup>10</sup>

## 2.2. Acceleration

One of the most distinctive features in FFAG accelerators compared with ordinary strong focusing synchrotrons is that very fast acceleration can be allowed because the magnetic field is static. Accordingly, various new RF

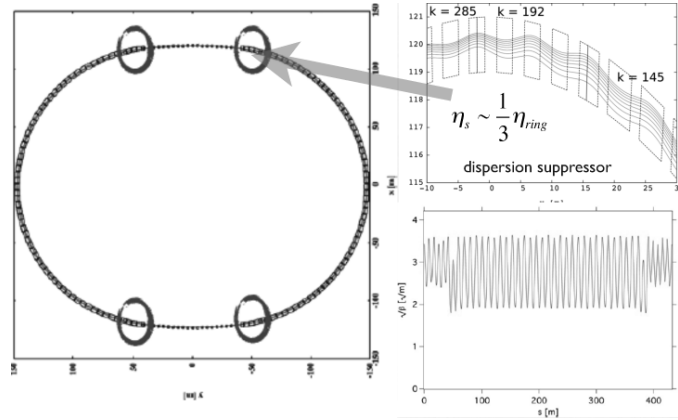


Fig. 2. Scaling FFAG for muon acceleration with dispersion suppressing insertions.

acceleration schemes, which are adequate either or both for scaling and non-scaling FFAG accelerators, have been proposed for fast acceleration, and some of them have already been realized.

### 2.2.1. Broad-band RF cavity with MA cores

Broad-band RF cavities with high permeability magnetic alloy (MA) cores have been used mostly in scaling type of proton FFAG accelerators such as the POP-FFAG developed at KEK. No frequency tuning synchronized with beam revolution is needed and a very rapid acceleration cycle of several 100Hz to 1kHz becomes possible, however, above than that, it seems rather difficult with the practical rf voltage obtained by this type of rf cavity.

### 2.2.2. Stationary RF bucket acceleration

In longitudinal phase space, RF bucket of the scaling type of FFAG accelerator for relativistic particles such as high energy muons is not distorted for large momentum range because the momentum compaction keeps constant and has no momentum dependence. If the RF voltage is large enough, the particles can be accelerated in a stationary RF bucket after a half period of synchrotron oscillation.<sup>11</sup>

### 2.2.3. Serpentine acceleration

In the non-scaling FFAG accelerator, a fixed frequency RF system is installed and acceleration out of longitudinal buckets can be possible for relativistic particles when the path length difference has a parabolic dependence on momentum as described above. The revolution time (time-of-flight per turn) changes and has a minimum during beam acceleration. Figure 3 shows an example of serpentine acceleration.<sup>12</sup>

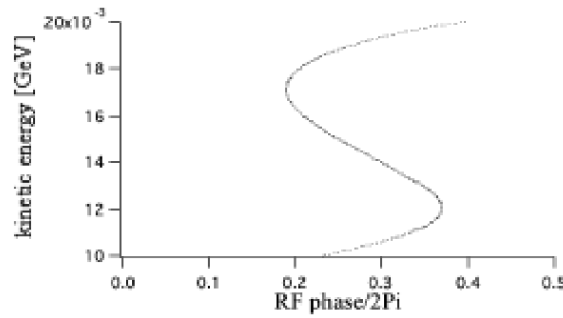


Fig. 3. Serpentine acceleration in non-scaling FFAG

In the scaling FFAG accelerator, the similar acceleration scheme with a fixed frequency RF is possible where the beam is accelerated passing through the transition energy where the time-of-flight per turn can be minimum. The longitudinal Hamiltonian in the case of scaling FFAG accelerator can be analytically obtained as,

$$\frac{H}{m_0 c^2 f_s} = 2\pi \left[ -\frac{A}{2(1-\lambda)} (\gamma^2 - 1)^{1-\lambda} + \gamma \right] + \frac{eVh}{m_0 c^2} \cos\phi. \quad (10)$$

Here,

$$\lambda = \frac{k}{2(k+1)} \quad (11)$$

$$A = \frac{(\gamma_s^2 - 1)^\lambda}{\gamma_s} \quad (12)$$

Figure 4 shows an example of the phase space contour for the longitudinal motion of the scaling FFAG accelerator. As can be seen from this figure, the serpentine path through the transition energy exists and beam

acceleration for non-relativistic particles can be possible with this scheme in scaling FFAG accelerator.

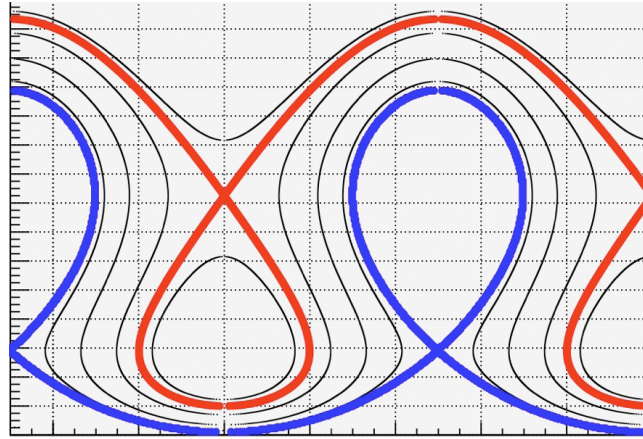


Fig. 4. Longitudinal Hamiltonian contour for serpentine acceleration in scaling FFAG accelerator.

#### 2.2.4. Harmonic number jump

In FFAG accelerators, the transverse beam positions change during acceleration. If the energy gain varies properly with transverse position to achieve an integer change in the harmonic number with each turn, the beam can be accelerated with a fixed frequency RF system.<sup>13</sup> The difficulty of this scheme is how to vary the energy gain properly and ideas such as a position dependent RF voltage configuration have been proposed to overcome this difficulty.

### 3. FFAG for high intensity proton accelerator

Next generation of high intensity proton accelerator (HIPA) is, needless to say, a proton driver for producing an order of magnitude more intense secondary particles such as neutron, muon, meson etc. compared with the present HIPA such as J-PARC, SNS and ISIS. Obviously, the beam energy of next generation HIPS should be more than 1GeV because the nuclear interaction generating hadron shower can be very efficient there and the beam power of more than 10MW is now under discussion. Requirements for the time structure of the beam from next generation HIPS, however, have so

many varieties which depend on each application. Neutrino factory/muon collider requires a very short beam bunch ( nsec) and low repetition rate operation ( 10Hz), on the other hand, ADSR requires very large repetition rate of more than KH or even cw operation. It must be favorable that next generation HIPS should satisfy these various requirements as much as possible.

The types of accelerator for next generation of HIPA, from this point of view, are limited. Ordinary synchrotron and cyclotron could be excluded as next generation of HIPS. The former is difficult for high repetition operation and the latter for short bunched and high peak intensity pulse operation. The candidates of the next generation HIPS could be a super conducting H- linac + proton storage ring (LINAC+PSR), and a FFAG.proton accelerator. The FFAG accelerator could be operated in various repetition pulsed mode and even in cw mode as described in the previous section.

Obviously, when the beam repetition is less than 1kHz, the braod-band RF system as described in the previous section can be used for either scaling or non-scaling FFAGs. However, in order to realize cw operation, fixed-frequency RF acceleration scheme is essential and, in particular, for the proton driver where the particle velocity is still non-relativistic, a scaling FFAG accelerator with serpentine acceleration seems to be a good candidate. Table 1 presents an example of parameter list of proton driver based on scaling FFAG accelerator using serpentine beam acceleration shown in Fig. 5.

Table 1. Parameters of an example of proton driver based on scaling FFAGs with serpentine acceleration

Item	Value
average radius(m)	15
field index	3
injection energy	300MeV
extraction energy	2.2GeV
RF voltage per turn (h=1)	38MV

#### 4. First ADSR experiment with FFAG accelerator at Kyoto University Research Reactor Institute (KURRI)

The Research Reactor Institute of Kyoto University started the KART (Kumatori Accelerator-driven Reactor Test facility) project in fiscal year

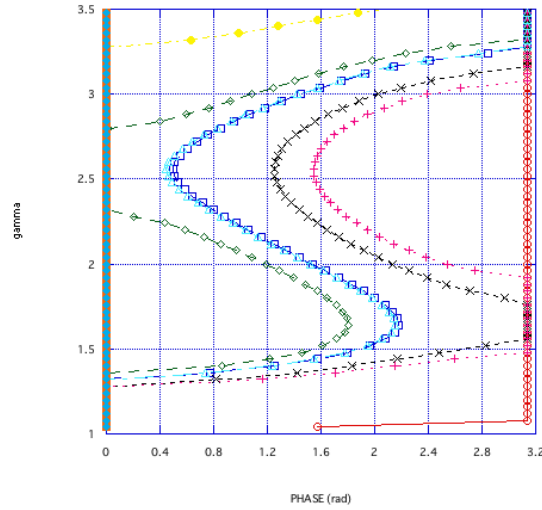


Fig. 5. Serpentine acceleration for HIPA(0.3-2.2GeV) with scaling FFAG accelerator.

2002 under the Contract with the Ministry of Education, Culture, Sports, Science and Technology of Japan and in March of 2009,<sup>14</sup> the first experiment of Accelerator-Driven Sub-critical Reactor system (ADSR) with the Kyoto University Critical Assembly (KUCA) has been successfully carried out. The purpose of this research project is to demonstrate the basic feasibility of accelerator-driven system (ADS), studying the effect of incident neutron energy on the effective multiplication factor in a subcritical nuclear fuel system. For this purpose, a variable-energy FFAG (Fixed Field Alternating Gradient) accelerator complex was developed and constructed, and coupled with the Kyoto University Critical Assembly (KUCA).<sup>15</sup> On March 4th, 2009, the world's first injection of spallation neutrons generated by the high-energy proton beams into a reactor core was successfully accomplished. By combining the Fixed Field Alternating Gradient (FFAG) accelerator (Fig. 6) with the A-core (Fig. 7) of KUCA, a series of ADSR experiments was carried out under the condition that the spallation neutrons were supplied to a subcritical core through the injection of 100 MeV protons onto a tungsten target, whose size was 80 mm diameter and 10 mm thickness.



Fig. 6. FFAG accelerator complex at KURRI.

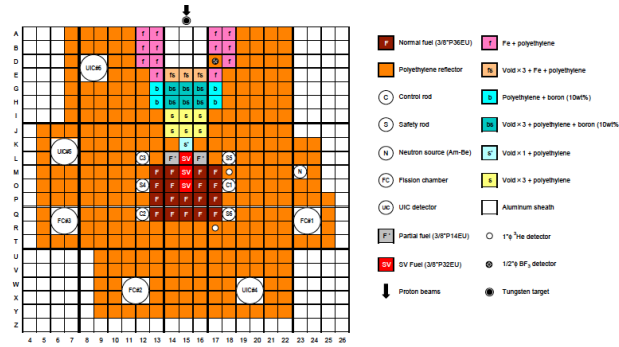


Fig. 7. A-core of KUCA at KURRI.

The accelerator complex is composed of three FFAG rings; injector, booster, and main ring.<sup>16</sup> The specifications of the each FFAG are summarized in Table 1. As a first stage, the accelerator complex has been planned to output 100 MeV-0.1 nA proton beams. The injector is a spiral type of scaling FFAG accelerator which is composed of eight spiral sector magnets, two acceleration gaps, and electric septa for injection and extraction, respectively. The field distribution in the radial direction can be controlled by trim-coils, and which makes variable energy acceleration possible. Maximum beam energy is 2.5 MeV in design. The booster FFAG is a radial sector type of scaling FFAG accelerator, which adopts multi-turn beam injection using horizontal space. The beam repetition rate is 60 Hz. For such a rapid-cycling accelerator, adiabatic capture cannot be used because relatively long beam capture time compared to the period of the synchrotron

oscillation is required. Thus, fast longitudinal matching with bunch rotation method was tried. Saw-tooth rf was employed in order to minimize the filamentation. The main ring is also a radial-sector type of scaling FFAG and its design is essentially same with the one that was developed at KEK in 2004. Proton beam of 11.6 MeV was injected in the main ring. The injected beam is kicked into the closed orbit by an electrostatic septum and a magnetic kicker. Figure 5 shows the circulating beam picked up by an electrostatic bunch monitor in the main ring. The betatron-phase advance between the kickers is 550 deg, so that the kickers work on phase. This means that the strengths of them is complementary. The beam was accelerated with the rf gap-voltage of 2.5 kV and the synchronous phase of 30 degree. A rapid beam-loss was observed at 4 ms at 20-25 MeV. The beamloss is related to  $\nu_x - 2\nu_y = 1$ . Figure 8 shows the measured betatron tune trajectory in the main ring during beam acceleration. The beam was successfully accelerated up to 100MeV with the beam current of more than 0.1nA and extracted and transported to the KUCA core. The beam current at the target placed in the KUCA core was about 10pA.

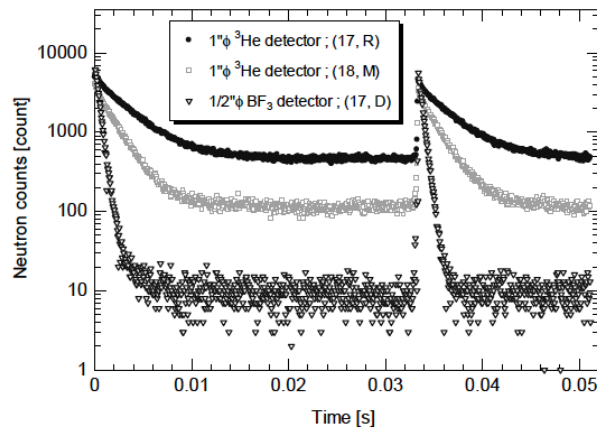


Fig. 8. Measured betatron tune trajectory during beam acceleration in the main ring.

The A-core employed in the ADSR experiments was essentially a thermal neutron system composed of a highly enriched uranium fuel and the polyethylene moderator/reflector. In the fuel region, a unit cell is composed of a 93 % enriched uranium fuel plate 1/16" thick and polyethylene

plates 1/4" and 1/8" thick. In these ADSR experiments, three types of fuel rods designated as the normal, partial and special fuel were employed. From the reason of the safety regulation for KUCA, the tungsten target was located not at the center of the core but outside the critical assembly, and an outside-location was similar to the previous experiments using 14 MeV neutrons. To obtain the information on the detector position dependence of the prompt neutron decay measurement, the neutron detectors were set at three positions shown in Fig. 6: near the tungsten target (Position of (17, D) experimentally confirmed by observing the time evolution of neutron density in ADSR: an exponential decay behavior and a slowly decreasing one, respectively. These behaviors clearly indicated the fact that the neutron multiplication was caused by an external-source: the sustainable nuclear chain reactions were induced in the subcritical core by the spallation neutrons through the interaction of the tungsten target and the proton beams from the FFAG accelerator. In these kinetic experiments, the subcriticality was deduced from the prompt neutron decay constant by the extrapolated area ratio method. The difference of measured results of 0.74 %  $\Delta k/k$  and 0.61 %  $\Delta k/k$  at the positions of (17, R) and (18, M) in Fig. 2, respectively, from the experimental evaluation of 0.77 %  $\Delta k/k$ , which was deduced from the combination of both the control rod worth by the rod drop method and its calibration curve by the positive period method, was within about 20 % . Note that the subcritical state was attained by a full insertion of C1, C2 and C3 control rods into the core. The generation of the spallation neutrons was included in the MCNPX calculation bombarding the tungsten target with 100 MeV proton beams. Since the reactivity effect of the In wire is considered to be not negligible, the In wire was taken into account in the simulated calculation: the reaction rates were deduced from tallies taken in the In wire setting region. The result of the source calculation was obtained after 2,000 active cycles of 100,000 histories, which led the statistical error in the reaction rates of less than 10 % . The measured and the calculated reaction rate distributions were compared to validate the calculation method. The calculated reaction rate distribution (Fig. 3) agreed approximately with the experimental results within the statistical errors in the experiments, although these experimental errors were rather larger than those of the calculations. These larger errors in the experiments were attributed to the current status of the proton beams, including the weak beam intensity and the poor beam shaping at the target.

## 5. Summary

Beam focusing and acceleration in Fixed Field Alternating Gradient Accelerator (FFAG) have been briefly described and a possible concept of FFAG accelerator for next generation High Intensity Proton Accelerator (HIPA) is discussed. The first experiment of ADSR with FFAGs at KURRI is also presented.

## References

1. T.Ohkawa, Proc. annual meeting of JPS(1953).
2. K.R.Symon et al., Phys. Rev 103,,1837(1956).
3. Y.Mori, Proc. EPAC1998,,289(2000).
4. A.A.Kolomenski, "Theory of Circular Accelerators", 340(1966).
5. D.Trbojevic, Proc. of the International Workshop on FFAG Accelerators (FFAG05), Osaka, Japan(2005).
6. G.Rees, Proc. of the International Workshop on FFAG Accelerators (FFAG04), Tsukuba, Japan, 2004,page 77.
7. A.G. Ruggeiero, Proc. of the International Workshop on FFAG Accelerators (FFAG05), Osaka, Japan, 2005, page 47.
8. JB.Lagrange, Proc. of PAC09, FR5PFP002, Vancouver, 2009.
9. Y.Mori, talk at the International Workshop on FFAG Accelerators(FFAG09) at FNAL, Chicago, USA, 2009.
10. T.Planche, Proc. of PAC09, FR5PFP003, Vancouver, 2009.
11. Y.Mori, talk at the International Workshop on FFAG Accelerators(FFAG2006) at FNAL, Chicago, USA, 2006.
12. S.Machida, Proc. of the International Workshop on FFAG Accelerators (FFAG05), Osaka, Japan, 2005, page 68.
13. S.Berg, Proc. of the International Workshop on FFAG Accelerators (FFAG05), Osaka, Japan, 2005, page 93.
14. K.Mishima et al, "Research Project on Accelerator-driven Subcritical System Using FFAG Accelerator and Kyoto University Critical Assembly" , J. Nucl. Scie. Technol., 44, 499(2007).
15. C.H.Pyon et al., "First Injection of Spallation Neutrons Generated by High-Energy Protons into the Kyoto University Critical Assembly", J. Nucl. Scie. Technol. rapid communication, (2009).
16. Y. Mori, "Development of FFAG accelerators and their applications for intense secondary particle production", Nucl. Instrum. Methods, 562 , 591, (2006).